

# Relating the attrition behaviour of crystals in a stirred vessel to their mechanical properties

Marco Bravi, Sergio Di Cave, Barbara Mazzarotta\*, Nicola Verdone

*Dipartimento di Ingegneria Chimica, Università di Roma "La Sapienza", Via Eudossiana 18, 00184 Rome, Italy*

Accepted 29 January 2003

## Abstract

The attrition behaviour of eight different crystalline materials in a stirred vessel was investigated applying similar fluid dynamic conditions, i.e. just suspending the crystals off-bottom. Despite the rather gentle stirring, all crystalline materials underwent remarkable attrition, generating, in 1 h, an amount of fragments ranging from 3.9 to 28.7% of the original mass. The attrition behaviour of the crystals was characterised basing on the size distribution of the fragments, which was analysed and modelled, confirming that they were mainly produced by abrasion mechanism. The morphological analysis of the fragments showed that the size of the main axes of the coarse residue got closer, while the fragments became more elongated as their size decreased. Two different approaches relating the attrition resistance of the materials to their hardness and to their stress resistance were examined and discussed in order to relate the attrition behaviour to the mechanical properties of the materials.

© 2003 Elsevier Science B.V. All rights reserved.

*Keywords:* Attrition behaviour; Crystallisation; Hardness

## 1. Introduction

Attrition consists in the generation of fragments from particles suspended in a fluid stream caused by their collisions, mutual and with fixed and/or mobile parts of the equipment. Attrition may occur according to the breakage mechanism, when the collision energy is significantly higher than that required for particle fracture, or the abrasion mechanism, when the collision energy is only capable of removing small amounts of material from the surface of the particle [1]. The consequences of such collisions are multi-fold, in that they reduce the value of the average particle size, change the particle size distribution and modify the particle morphology.

Crystallisation processes are particularly prone to attrition due to the intrinsic fragility of crystalline materials and to the agitation required to improve homogeneity and heat and mass transfer [2]. Moreover, some specific fragment generation mechanisms, such as initial breeding and needle breeding, associated to the detachment of crystalline dust or dendrites from the crystals, respectively, have been identified [3].

The study of the influence of the operating conditions on the attrition phenomena occurring during crystallisation processes has been the object of a great deal of work reported in the literature in the past years (see, for example [2,4–8]). Most of the published work actually concerns the influence of parameters such as time, stirring intensity, crystal size and concentration, and super saturation on fragment generation rate or on their size distribution or habit.

The present work addresses the comparison of the attrition behaviour of different crystalline materials exposed to similar fluid dynamic conditions, through the modelling of the size distribution and the morphological characterisation of the fragments, with the aim of relating the attrition resistance of the crystalline materials to their mechanical properties.

## 2. Attrition experiments

The experiments were performed on commercial product of purity higher than 99% by weight supplied by Aldrich. Eight different organic and inorganic materials, characterised by crystal densities ranging from 1396 to 2662 kg/m<sup>3</sup> were considered. The main characteristics of the products are summarised in Table 1. The crystals were preliminarily sieved determining, for each product, the size range

\* Corresponding author. Tel.: +39-06-44585-590; fax: +39-06-4827453.  
E-mail address: mazzarot@ingchim.ing.uniroma1.it (B. Mazzarotta).

### Nomenclature

$A$	area of the particle ( $\text{m}^2$ )
$E$	Young modulus (Pa)
$E_c$	kinetic energy of the crystals (J)
$E_p$	energy required to crush the crystals (J)
$F$	compression load at fracture (N)
$H_v$	Vickers hardness (Pa)
$k_b$	fraction of fracture due to breakage mechanism
$K_v$	parameter of Eq. (8)
$L$	fragment size (mm)
$L_{\max}$	maximum initial size of the crystals (mm)
$n_b$	modulus of Broadbent–Callcott size distribution of breakage fragments
$P$	perimeter of the particle (m)
$v$	velocity (m/s)
$W_c$	critical work to form cracks (J)
$x$	dimensionless size ( $L/L_{\max}$ )
$x_r$	dimensionless size of the smallest coarse abrasion residue
$x_f$	dimensionless size of the largest fine abrasion fragment
$y_w$	cumulative weight fraction of fragments
$y_{w,af}$	cumulative weight fraction of fine abrasion fragments
$y_{w,ar}$	cumulative weight fraction of coarse abrasion residue
$y_{w,b}$	cumulative weight fraction of breakage fragments
$y_{wf}$	cumulative weight fraction of fine fragments
$z_d$	deformation from loading point (m)

### Greek letters

$\beta$	aspect ratio of the particle (width/length)
$\rho_c$	crystal density ( $\text{kg/m}^3$ )
$\sigma$	stress resistance (Pa)
$\Phi$	roundness ( $\Phi = P^2/4\pi A$ )

representative of the average crystal size. The fraction falling into this size range was collected and used for the experiments. The average crystal size of the products were in the range 0.25–0.85 mm.

The experimental apparatus was a 200 mm-diameter cylindrical vessel, described in detail elsewhere [9], fitted with four radial baffles and stirred by a 75 mm-diameter marine propeller.

The attrition runs were carried out at room temperature, dispersing the crystals into xylene, which was demonstrated to be a non-solvent liquid for all the materials from preliminary solubility tests. These were carried out for each product by stirring a 30 ml suspension containing excess crystals for 24 h, then withdrawing a sample of the liquid and placing it into an oven at 80 °C for 24 h. The liquid evaporated completely and no trace of solid matter was detected in the sample vessel.

The attrition experiments were performed at a suspension density of 100  $\text{kg/m}^3$ ; each run consisted in keeping 500 g of crystals suspended in 5 l of xylene by stirring for 1 h. After discharging and filtering the whole suspension under vacuum using a Whatman no. 3 filtering paper, the recovered crystals were dried and sieved down to 63  $\mu\text{m}$  to determine their size distribution. Crystal losses during these operations were within 0.5 wt.% for all runs and temperature fluctuations were limited to 1 °C. Most of the runs were duplicated obtaining a very good reproducibility of the particle size distribution.

The use of non-solvent media in attrition experiments has been suggested [2] to avoid the simultaneous occurrence of other phenomena, such as primary nucleation and growth, also capable of modifying the crystal size distribution and habit. Moreover, attrition was found to generate a larger number of nuclei in non-solvent media than in regular aqueous solutions, probably due to agglomeration phenomena which are more likely in the latter [10]. On the other hand, most information derived from experiments in non-solvent media can be extended to crystallisation processes carried out in supersaturated solutions [11].

In order to properly compare the attrition behaviour of crystals different for both size and density, the stirring modalities were carefully selected to ensure that the fluid dynamic conditions were as similar as possible. In particular, the stirring rate was set to a value just above the minimum solid off-bottom suspending velocity for each investigated product. The values of this velocity, defined according to the Zwietering criterion as that at which the

Table 1  
Crystal properties and operating conditions of the attrition runs

Crystalline material	Density ( $\text{kg/m}^3$ )	Size (mm)	Habit	Roundness	Aspect ratio	$N$ (rps)
Citric acid	1542	0.5–0.6	Monoclinic	1.21	0.76	11.67
Pentaerythritol	1396	0.5–0.6	Tetragonal	1.20	0.82	10.00
Potassium chloride	1988	0.25–0.3	Cubic	1.23	0.75	13.33
Potassium sulphate	2662	0.355–0.425	Orthorhombic	1.26	0.73	16.67
Sodium chloride	2163	0.355–0.425	Cubic	1.27	0.75	15.00
Sodium perborate	1730	0.425–0.5	Dendritic	1.31	0.81	13.33
Sodium sulphate	1490	0.71–0.85	Monoclinic	1.17	0.70	11.67
Sucrose	1585	0.355–0.425	Monoclinic	1.39	0.77	11.67

Table 2  
Overall attrition and values of the parameters of the model

Crystalline system	Fragments (%)	$x_f$	$x_r$	$y_{wf}$	$k_b$	$n_b$
Citric acid	13.7	0.22	0.64	0.0031	0.0459	2.9
Pentaerythritol	15.1	0.28	0.60	0.0012	0.0163	2.6
Potassium chloride	11.7	0.39	0.64	0.0016	0.0968	5.8
Potassium sulphate	3.9	0.32	0.79	0.0031	0.0473	4.2
Sodium chloride	7.7	0.29	0.55	0.0003	0.0055	2.7
Sodium perborate	12.6	0.20	0.73	0.0078	0.0439	3.0
Sodium sulphate	8.8	0.61	0.83	0.0701	0.0274	3.8
Sucrose	28.7	0.45	0.53	0.0012	0.0001	5.0

crystals do not rest on the bottom longer than 1–2 s [12], were preliminarily calculated with the Zwietering relationship and then checked during the experiments, finally setting the values listed in Table 1. The power number of the impeller, equal to 0.685, was determined from torque measurements. Accordingly, the stirring power for the examined products was in the range 0.3–1.45 W/kg which are usual values for crystallisation processes.

The set of operating conditions selected for each system is expected to correspond to the occurrence of all the types of collisions (crystal–crystal, crystal–vessel, crystal–impeller) which usually contribute to crystal attrition [13].

The morphology of the crystals and of the fragments was investigated by submitting 10–20 crystals belonging to each size fraction to image analysis, using an OLYMPUS optical microscope connected to a LEICA image acquisition system. The measurements were repeated on two to three different samples of each size fraction, then taking the average value.

The roundness, defined as:

$$\Phi = \frac{P^2}{4\pi A} \quad (1)$$

and the aspect ratio  $\beta$  (width/length ratio), were selected as the main morphological parameters. The former points to excess in perimeter, as those arising from the presence of dendrites, while the latter indicates how elongated the particle is. The values of roundness and aspect ratio of the crystals used in the experiments are listed in Table 1.

### 3. Results and discussion

#### 3.1. Overall amount of fragments

In spite of the rather gentle stirring conditions, all the investigated materials underwent significant attrition. The overall amount of fragments smaller than the original crystals ranged from 4 to 28 wt.% for the eight investigated products (see Table 2). The highest values were obtained for sucrose, pentaerythritol and citric acid, while the lowest for potassium sulphate, sodium chloride and sodium sulphate.

In principle, the amount of fragments depends on the impact energy and on the number of impacts and, operating at

fixed solid concentration, it should increase with the square of the stirring rate, the cube of the crystal size and the crystal density [2]. On this basis, the lowest amounts of fragments were expected from potassium chloride and sucrose and the highest from sodium sulphate and potassium sulphate. The experimental results are not in this order, indicating that, under similar fluid dynamic conditions, the attrition resistance of the crystals mainly depends on some intrinsic property of the materials.

#### 3.2. Size distribution of the fragments

The final size distributions of the attrition product, expressed as cumulative mass fraction  $y_w$  versus dimensionless size  $x$  ( $x = L/L_{\max}$ ), are compared in Fig. 1, where logarithmic scales are used to properly examine also the small size fragments zone. It can be observed that each investigated material presents a characteristic trend of the size distribution curve, which may be regarded as an index of its attrition behaviour. However, in all cases, the sizes of the fragments ranged from values just below those of their parent crystals to less than 63  $\mu\text{m}$ . The slight slope of the cumulative curve for fragment sizes ranging from 30 to 60% those of their parent crystals, indicates that breakage mechanisms also gives a contribution to overall attrition. In fact, breakage is assumed to cause the fracture of the parent crystal into a number of relatively large pieces, while abrasion is assumed to produce a localised fracture of the parent crystal, which is just slightly damaged, generating, at the same time, a number of much smaller fragments.

The cumulative size distribution curves of the fragments also give some indication about the attrition resistance of the investigated products, since higher  $y_w$  values imply a greater generation of fragments. Due to the different trends of the curves, their relative position changes with the

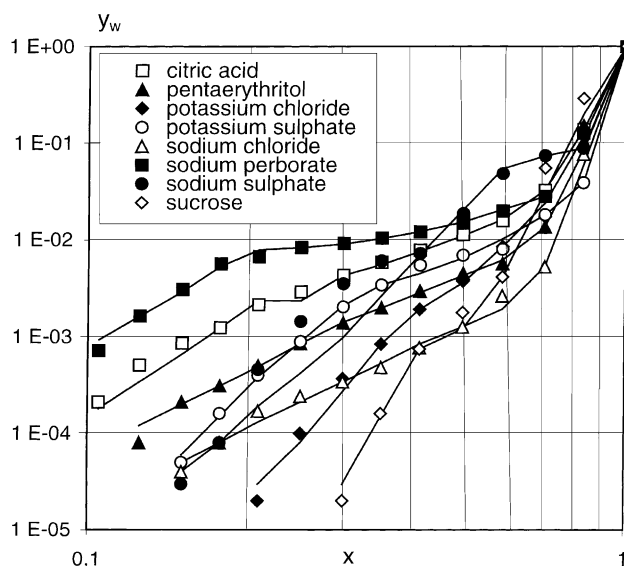


Fig. 1. Final size distribution of the attrition fragments.

abscissa value; however, sodium chloride, sucrose and potassium chloride appear to generate less fragments than sodium sulphate, sodium perborate and citric acid. It may be worth noting that this attrition resistance scale is quite different from that obtained basing on the total amount of generated fragments.

The crystal attrition model proposed by Mazzarotta [5] was applied to fit the cumulative fragment size distribution curves. It takes into account the occurrence of both abrasion and breakage attrition and makes use of the following assumptions: (i) breakage generates fragments  $y_{w,b}$  in the whole dimensionless size range  $0 < x < 1$ ; (ii) abrasion generates small fragments,  $y_{w,af}$  of size below the dimensionless value  $x_f$  and leaves a coarse residue,  $y_{w,ar}$  larger than the dimensionless size  $x_r$ ; (iii) the cumulative mass size distribution of the attrition fragments  $y_w$  can be obtained by linearly combining the size distributions of the fragments generated by abrasion and breakage by means of the parameter  $k_b$ , contribution of breakage mechanism to overall attrition ( $k_b \leq 1$ ):

$$y_w = k_b y_{w,b} + (1 - k_b)(y_{w,af} + y_{w,ar}) \quad (2)$$

where  $(1 - k_b)$  is the contribution of abrasion; (iv) the cumulative mass fractions of the fragments

$$y_w = \frac{1 - \exp(-x)^n}{1 - \exp(-1)^n} \quad (3)$$

can be evaluated from the Broadbent–Callcott size distribution [14], where  $n$  is the distribution modulus. Eq. (3) applies to fine ( $y_{w,b}$ ,  $n_f$ ) and coarse ( $y_{w,ar}$ ,  $n_r$ ) abrasion fragments and to breakage fragments ( $y_{w,b}$ ,  $n_b$ ). Taking into account the congruity condition (abrasion does not generate fragments in the dimensionless size range  $(x_f - x_r)$ :

$$x_{w,af}(x_f) = x_{w,ar}(x_r) \quad (4)$$

and defining the overall mass fraction of fine fragments (generated both by abrasion and breakage mechanism)  $y_{wf}$ , as

$$y_{wf} = k_b y_{w,b}(x_f) + (1 - k_b) y_{w,af}(x_f) \quad (5)$$

the model contains five independent parameters (for details see [5]):  $x_f$ , dimensionless size of the largest abrasion fragment;  $x_r$ , dimensionless size of the coarsest abrasion residue;  $k_b$ , fraction of breakage attrition;  $n_b$ , modulus of the Broadbent–Callcott distribution of breakage fragments;  $y_{wf}$ , overall mass fraction of fragments smaller than  $x_f$ . The values of the parameters, determined by fitting the experimental size distribution of the fragments using the regression procedure reported in [15], are listed in Table 2; the fitting, shown in Fig. 1, appears excellent, also due to the limited number of data of some curves.

The values assumed by the parameters of the models also allow to draw some considerations about the attrition mechanism and the attrition resistance. First, the absolute values of  $k_b$  confirm that abrasion is the prevailing fracture mechanism in stirred crystallisers [5,8,9]. In fact, breakage fracture

contributes to 0.01–9.7% of total attrition for all the investigated products. The overall fraction of fine fragments  $y_{wf}$  gives a partial measurement of the attrition suffered by the material, especially when combined with the fraction of the attrition associated to breakage mechanism,  $k_b$ . In fact, low values of both  $k_b$  and  $y_{wf}$  are a clear index of good attrition resistance, as in the case of sodium chloride and sucrose; on the contrary, rather high values of  $k_b$  do not correspond to a worse attrition resistance when coupled with a low  $y_{wf}$  value, as occurs for potassium chloride.

### 3.3. Fragments morphology

Also, the morphology of the fragments can give useful information about the attrition behaviour of the investigated products. The values of the roundness and of the aspect ratio of the parent crystals are listed in Table 1. The former is an index of the sphericity of the particle, which increases as the value of this parameter approaches unity; the latter is an index of the elongation of the particle, which decreases as the value of this parameter approaches unity. By combining this information, it can be observed that neither sodium perborate nor sucrose parent crystals are very spherical (see Table 1), but that the former are actually quite elongated, while the latter are not. As a matter of fact, the direct microscope observation of the sucrose crystals clearly showed that some agglomeration had occurred during the production process, therefore, this agglomeration is actually the cause of their high roundness value (as well as the most likely cause of the very high value of the overall amount of fragments previously observed).

The fragments belonging to all the size ranges were also submitted to morphological analysis: all of them appeared as individual particles and no trace of agglomeration was detected. The obtained trends of roundness and aspect ratio versus the dimensionless size  $x$  are shown in Figs. 2 and 3 for some of the examined products. First it should be remarked that both the roundness and the aspect ratio of the attrition fragments belonging to the parent crystal size range (i.e. the coarsest residue) were generally higher than those of the original crystals. Accordingly, attrition makes closer the two main axes of the crystals still belonging to the parent size range, even if the particle results less spherical. On the contrary, the generated fragments become more elongated as their size decreases; for most materials the roundness does not vary appreciably with size, while for others, such as citric acid, it increases remarkably at the smallest sizes. Based on morphological analysis it can be assumed that crystal fracture occurs along preferential planes, possibly following the path of pre-existing cracks, with the detachment of tiny elongated fragments. This general behaviour is in agreement with previous observations [8].

The actual extent of the variation of the aspect ratio with the crystal size depends on the examined products, being minimum for sodium chloride, and maximum for citric acid.

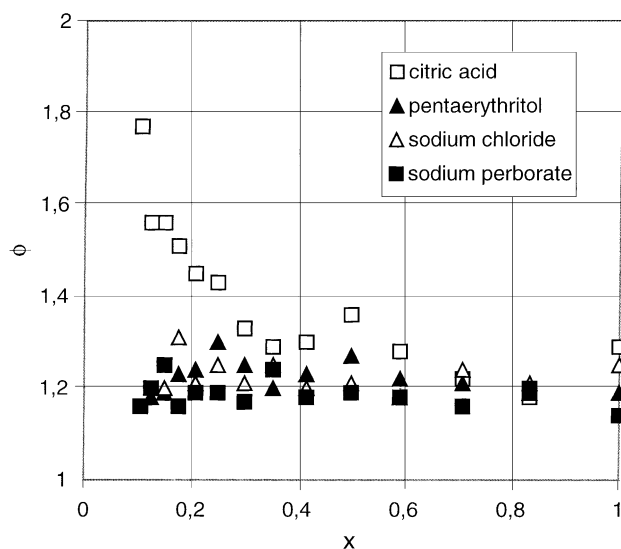


Fig. 2. Roundness of the attrition fragments.

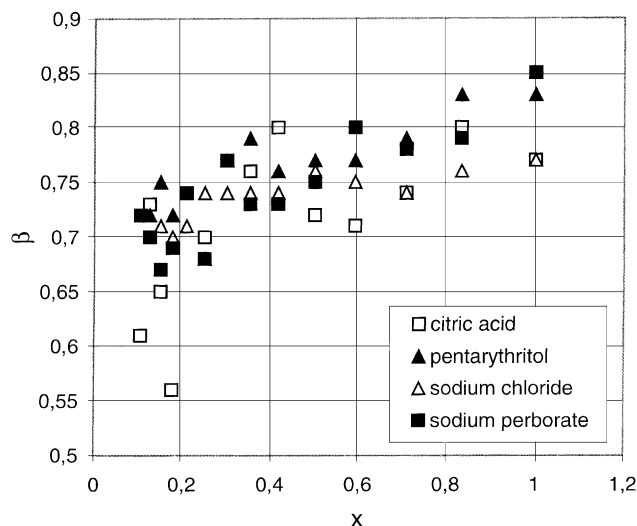


Fig. 3. Aspect ratio of the attrition fragments.

It is interesting to note that the products previously found to be among the most resistant to attrition also appear to be those which suffer the least from habit modifications and vice versa.

Table 3  
Kinetic energy and mechanical properties of the crystals

Crystalline system	$H_v$ (MPa)	$W_c$ (J)	$E_c$ (J)	$E$ (GPa)	$F$ (N)	$\sigma$ (MPa)
Citric acid	454	$3.5 \times 10^{-9}$	$9.7 \times 10^{-7}$	–	0.79	2.24
Pentaerythritol	–	–	$6.5 \times 10^{-7}$	–	0.89	2.67
Potassium chloride	91	$>1 \times 10^{-3}$	$2.0 \times 10^{-7}$	18.1	0.78	11.78
Potassium sulphate	1502	$3.0 \times 10^{-9}$	$1.22 \times 10^{-6}$	31.9	0.90	3.96
Sodium chloride	166	$>8 \times 10^{-4}$	$8.0 \times 10^{-7}$	24.9	0.85	5.83
Sodium perborate	–	–	$8.4 \times 10^{-7}$	–	0.77	3.80
Sodium sulphate	–	–	$2.67 \times 10^{-6}$	–	1.67	2.69
Sucrose	–	–	$3.6 \times 10^{-7}$	–	0.83	5.29

#### 4. Attrition resistance and mechanical properties of the crystals

Attrition occurring during the operation of crystallisers is due to impacts between the suspended solids, the still and moving parts of the equipment and the crystals themselves. Among these events, the impacts between the crystals and the impeller tips occur with the highest energy. When the absolute value of this energy is low, an elastic deformation of the crystal occurs but, as the impact energy increases, first the resistance of some spots on the crystal surface is overcome, causing abrasion fracture, then the resistance of the whole crystal is exceeded, and the crystal is shattered according to the breakage mechanism.

Accordingly, the knowledge of the mechanical properties of the crystalline material appears of the greatest importance, even if very limited experimental data seem to be available in the literature. The main source of information is given by hardness measurements, performed by Vickers indentation on a number of crystalline materials [16,17], while no stress resistance measurements appear to be reported.

In particular, Gahn and Mersmann [16] used the measured force applied to a Vickers diamond or a cone yielding a crack and the geometry of the formed indentation to calculate the critical work for crack formation. The investigated products also include four compounds used in the present work: citric acid, potassium sulphate, sodium chloride and potassium chloride. The values of the Vickers hardness,  $H_v$ , and that of the critical work to form cracks,  $W_c$ , determined by these authors [16] are listed in Table 3. It can be noted that the hardest substances are also those requiring the lowest work to form cracks. The values of  $W_c$  are quite similar, and rather low, for citric acid and potassium chloride while they increase more than five orders of magnitude for sodium and potassium chloride. This scale is only in partial agreement with the attrition resistance observed in the present experiments; in fact, citric acid is very liable to attrition, while potassium and sodium chloride appear more resistant. However, it should be observed that potassium sulphate also exhibits a rather good attrition resistance, even if the reported value of the critical work to form cracks is low.

Gahn and Mersmann [16] remark that, for the majority of the crystalline substances object of their investigation, the work necessary to form cracks is orders of magnitude lower



than the impact energy usually experienced in crystallisers. This is not true in the present case, where the kinetic energy is below the work needed to form cracks for both sodium and potassium chloride. Despite this fact, these two products suffered attrition, even if to a more limited extent with respect to other ones. Gahn and Mersmann [16] also observed that the onset of cracks, during fast loading runs simulating the conditions found in agitated vessels, is possible at stress value well below that required for the same phenomenon in quasi-static runs, and postulated that this could be due to a lower dynamic hardness.

In the present work, a different approach to the problem of attrition resistance is proposed, basing on the evaluation of stress resistance of the material, comparing the impact energy to that required to crush the particles.

The impact energy can be assumed to be equal to the kinetic energy,  $E_c$ , of the crystals:

$$E_c = 0.5\rho_c L^3 v^2 \quad (6)$$

The values of the kinetic energy calculated for the average size of the parent crystals of each investigated material at the respective experimental conditions are listed in Table 3.

The energy required to crush a particle,  $E_p$ , can be calculated as the product of the loading compression,  $F$ , and the deformation from the loading point  $z_d$  [18]:

$$E_p = Fz_d \quad (7)$$

where the deformation is:

$$z_d = K_v \frac{F}{LE} \quad (8)$$

$K_v$  is a parameter dependent only on the Poisson's ratio and  $E$  the Young's modulus. Unfortunately, no value of the Poisson's ratio seems to be available for the investigated products, and the values of Young's modulus, listed in Table 3, are reported only for potassium chloride, sodium chloride and potassium sulphate [19].

In order to determine the stress resistance of the investigated materials, crush tests were performed on single crystals of each material, using a JJ Loyd Instrument, model T 20000, at an advancement rate of 0.0083 mm/s. Due to both the characteristics of the available instrument and to the very small size of the particles, the measurements required great experimental skill and the accuracy was not high ( $\pm 20\%$ ). The measurements were repeated five times for each product, obtaining the average values of the loading compression,  $F$ , listed in Table 3.

Based on the available information, and assuming that the value of the Poisson's ratio does not change for the investigated products (i.e. regarding  $K_v$  as a constant) it is possible to compare the  $E_c/F_p$  ratios, which increase in the order: potassium chloride, sodium chloride and potassium sulphate. Higher ratios are an index of easier fracture, and this scale appears in good agreement with the relative position of the final portion ( $x < 0.3$ ) of the attrition curves of the products under examination.

The values of the stress resistance,  $\sigma$ , calculated for each material by dividing the load at fracture by the undeformed cross-section are also listed in Table 3. It can be noted that the stress resistance scale appears in very good agreement with the attrition resistance one.

The above results clearly show that the attrition resistance of a material is related to its intrinsic mechanical properties, even if much more work is necessary before attempting to predict to which extent a material will undergo attrition phenomena from the sole knowledge of its mechanical characteristics.

## 5. Conclusions

Attrition experiments were carried out on eight crystalline products at just off-bottom suspension conditions to compare the attrition resistance of the materials. Despite the gentle stirring, in all cases a significant amount of fragments was generated, whose size spread from coarse to very fine. The prevailing attrition mechanism was abrasion, the length and the width of the damaged crystals still falling in the parent size range got closer, while the fragments became more elongated as their size decreased. Different attrition scales can be derived from the data, basing on the comparison of the overall amount of generated fragments or on the particle size distribution of the fragments at different sizes. These attrition scales were not found to be directly related to physical or operating parameters, such as the crystal density, the parent crystal size and the stirring rate, thus confirming that similar fluid dynamics conditions apply to all products. Approaches based on the mechanical properties of the materials, such as the critical work to form a crack, based on hardness measurements, and, especially on stress resistance measurements performed in crush tests, appear promising and should be further investigated in order to allow the prediction of the attrition behaviour for untested materials.

## Acknowledgements

The contribution of F. Cacciotti to the experimental work, of Prof. G. Rinaldi to the crush tests, and the financial support of MURST, Italy, is gratefully acknowledged.

## References

- [1] C.R. Bemrose, J. Bridgwater, Powder Technol. 49 (1987) 97–126.
- [2] A.W. Nienow, R. Conti, Chem. Eng. Sci. 33 (1978) 1077–1086.
- [3] R.F. Strickland-Constable, Kinetics and Mechanism of Crystallization, Academic Press, London, 1968.
- [4] P. Ayazi Smalou, A.G. Jones, K. Djamarani, Chem. Eng. Sci. 45 (1990) 1405–1416.
- [5] B. Mazzarotta, Chem. Eng. Sci. 47 (1992) 3105–3111.
- [6] A. Chianese, F. Di Berardino, A.G. Jones, Chem. Eng. Sci. 48 (1993) 551–560.

- [7] A. Chianese, R.G. Sangl, A.B. Mersmann, *Chem. Eng. Commun.* 146 (1996) 1–12.
- [8] B. Mazzarotta, S. Di Cave, G. Bonifazi, *AIChE J.* 42 (12) (1993) 3554–3558.
- [9] B. Mazzarotta, *AIChE Symp. Ser.* 89 (293) (1993) 112–117.
- [10] H. Offerman, J. Ulrich, *Ind. Crystal.* 8 (1982) 313–314; S.J. Jancic, E.J. de Jong (Eds.), North Holland Publishing Company, Amsterdam, 1992.
- [11] A. Chianese, N. Santilli, in: *Proceedings of the BIWIC 94*, Bremen, 8–9 September 1994, pp. 48–55.
- [12] T.N. Zwietering, *Chem. Eng. Sci.* 8 (1958) 244–253.
- [13] R. Conti, A.W. Nienow, *Chem. Eng. Sci.* 35 (1980) 543–547.
- [14] S.R. Broadbent, T.G. Callcott, *J. Inst. Fuel* 29 (1956) 524–539.
- [15] H.H. Rosenbrock, C. Storey, *Computational Techniques for Chemical Engineers*, Pergamon Press, London, 1966.
- [16] C. Gahn, A. Mersmann, *Powder Technol.* 85 (1995) 71–81.
- [17] J. Ulrich, M. Kruse, *J. Phys. D: Appl. Phys.* 26 (1993) 168–171.
- [18] E.G. Kelly, D.J. Spottiswood, *Introduction to Mineral Processing*, Wiley, New York, 1992, pp. 112–123.
- [19] Landolt-Bornstein, in: K.H. Hellwege (Ed.), *Numerical Data and Functional Relationships in Science and Technology*, Group 3, vol. 11, Springer, Berlin, 1979, p. 1.